Polymeric Carbon Nanocomposites From Multiwalled Carbon Nanotubes Functionalized With Segmented Polyurethane

Tzong-Liu Wang,[1] Ching-Guey Tseng[2]

[1]*Department of Chemical and Materials Engineering, National University of Kaohsiung, Kaohsiung 811, Taiwan, Republic of China*
[2]*Department of Chemical and Materials Engineering, National Kaohsiung University of Applied Sciences, Kaohsiung 807, Taiwan, Republic of China*

Received 9 January 2007; accepted 18 January 2007
DOI 10.1002/app.26224
Published online 25 April 2007 in Wiley InterScience (www.interscience.wiley.com).

ABSTRACT: Multiwalled carbon nanotubes (MWNT) were functionalized with segmented polyurethanes (PU) by the ''grafting to'' approach. Raman and X-ray photoelectron spectroscopy (XPS) spectra show that the sidewalls of MWNTs have been functionalized with acid treatment, and the amount of COOH increases with increasing acid treatment time. FTIR and X-ray diffraction (XRD) spectra confirm that PU is covalently attached to the sidewalls of MWNTs by esterification reaction. Similar to the parent PU, the functionalized carbon nanotube samples are soluble in highly polar solvents, such as dimethyl sulfoxide (DMSO) and *N*,*N*-dimethylformamide (DMF). The functionalized acid amount and the grafted PU amount were determined by thermogravimetric analyses (TGA). Comparative studies, based on SEM images between the PU-functionalized and chemically defunctionalized MWNT samples, also reveal the covalent coating character. Dynamic mechanical analysis (DMA) of nanocomposite films prepared from PU and PU-functionalized MWNTs show enhanced mechanical properties and increased soft segment T_g. Tensile properties indicate that PU-functionalized MWNTs are effective reinforcing fillers for the polyurethane matrix. © 2007 Wiley Periodicals, Inc. J Appl Polym Sci 105: 1642–1650, 2007

Key words: multiwalled carbon nanotubes; segmented polyurethanes; grafting to; nanocomposite; reinforcing fillers

INTRODUCTION

Carbon nanotubes (CNTs) have attracted interest since their discovery in 1991 because they exhibit fascinating electronic, thermal, and mechanical properties.[1,2] With extremely high mechanical strength and chemical stability, CNTs represent attractive possibilities for developing ultrastrong composite materials.[3,4] The effective utilization of CNTs in nanocomposite applications depends strongly on the ability to disperse the CNTs homogeneously throughout a matrix without destroying the integrity of the CNTs. However, the manipulation and processing of CNTs have been limited by their insolubility in most common solvents.[5] By functionalization or modification of nanosurfaces of CNTs, it has unlocked a new era in the development and applications of CNTs containing hybrid nanomaterials.[6–8] This can be generally fulfilled by the ''grafting to''[9–12] and ''grafting from''[13–16] approaches. Many potential applications of polymer-carbon nanotube composite materials have been proposed and discussed.[17–21] This may be attributed to that the individual properties of the two materials can be combined to give one novel hybrid nanomaterial with good mechanical strength, high thermal conductivity, and excellent processing ability.[15,22] The CNTs can offer a kind of nanosize reinforcement with a light weight, a hollow-core immerse aspect ratio, and an exceptionally high axial strength. Hence, significant efforts have been made in the fabrication of these nanocomposites by dispersing either single-walled (SWNT) or multiple-walled (MWNT) carbon nanotubes into various polymer matrices. Some experimental studies on CNT-reinforced polymer composites have been reported for various kinds of organic polymers, including polyethylene,[23,24] polypropylene,[25] poly(methyl methacrylate),[26,27] polystyrene,[28] pitch,[29] epoxy,[30,31] with enhanced mechanical and electrical properties. Recently, polyurea-functionalized CNTs have also been prepared via an *in situ* polycondensation approach.[32] However, Gao's approach could not be used in the preparation of segmented polyurethane elastomers (PUDs) functionalized carbon nanotubes, because PUDs must be prepared through a prepolymer

Correspondence to: T.-L. Wang (tlwang@nuk.edu.tw).

Journal of Applied Polymer Science, Vol. 105, 1642–1650 (2007)

technique. In addition, although Kim and coworkers reported dispersion of CNTs in a waterborne polyurethane matrix,[33,34] the dispersion of carbon nanotubes in the PUD matrix was only through a noncovalent solution blending. Elastomeric thermoplastic block copolymers are typically microphase-separation materatials containing two types of segments in their molecular architecture. To our knowledge, thermoplastic PUDs (i.e., segmented copolyurethanes or polyurethane block copolymers) functionalized CNTs nanohybrids via a covalent bonding have not been reported. It was expected PUDs functionalized CNTs nanohybrids would be more compatible with PUD matrices and hence could reinforce PUDs. Since polyurethane block copolymers are a class of high performance materials for versatile end use, nanocomposites prepared from PUDs reinforced with CNTs may extend its application in various fields.

In this article, we present a methodology to bind as-prepared segmented polyurethanes to CNTs via the ''grafting to'' approach. This work has been accomplished by the incorporation of carboxyl groups into the polyurethane backbone and the esterification reaction between functionalized CNTs and PU. The segmented polyurethanes with carboxyl groups pendant on the chain extender was synthesized by the conventional prepolymer technique. The functionalized CNTs and MWNT-PU nanohybrids have been characterized in detail to confirm the covalent linkage. In addition, results from the fabrication and characterization of the polyurethane-carbon nanotube nanocomposite films are presented and discussed.

EXPERIMENTAL

Materials

The MWNTs used in this work were purchased from Desunnano; the purity is higher than 95%. Thionyl chloride ($SOCl_2$) were obtained from Aldrich and used as received. 4,4′-Methylenebis(phenyl isocyanate) (MDI, Aldrich), methyl isobutyl ketone (MIBK, Hayashi Chemicals), *N*,*N*-dimethylformamide (DMF, Tokyo Chemicals), ethyl acetate (EA, Tokyo Chemicals), and dimethyl sulfoxide (DMSO, Nacalai Tesque) were distilled under reduced pressure. 2,2-Bis(hydroxymethyl) propionic acid (DMPA, Fluka) and tetrahydrofuran (THF, Tokyo Chemicals) were used as received. Poly(tetramethylene ether glycol) (PTMG, $\overline{M_n}$ = 1000) was degassed *in vacuo* at 55°C and 600 Pa (4.5 mmHg) for 3 h to remove any absorbed water. Nitric acid (EP grade), sulfuric acid (EP grade) was purchased from Nihon Shiyaku Industries, and used as received.

Synthesis of the segmented PUD

The preparation method of the segmented PUD carrying a carboxyl group in the chain extender is described in our previous article.[35] $\overline{M_n}$ and polydispersity determined by gel permeation chromatography are 90,400, and 1.68, respectively. The reaction is given in Scheme 1. For convenience, this polymer is designated as PUD.

Acid treatment of MWNTs

Typically, 1.0 g of crude MWNTs, 50 mL of 60% HNO_3, and 150 mL of 98% H_2SO_4 was added into a 500-mL flask equipped with a condenser with vigorous stirring. This mixture was then sonicated for 4 h at 40°C in an ultrasonic bath (40 kHz) to introduce carboxylic acid groups on the MWNTs surface. For comparison, experiments for acid treatment time of 8 and 24 h were also carried out. After cooling to room temperature, the reaction mixture was diluted with 200 mL of deionized water and then vacuum filtered through a filter paper (MFS). The solid was dispersed in 200 mL of water and filtered again, and then 100 mL of water was used to wash the filtrate several times. The dispersion, filtering, and washing steps were repeated until the pH of the filtrate reached 7. The filtered solid was then dried under vacuum for 24 h at 60°C. The MWNT-COOH was obtained in a 62% yield. The samples obtained from different acid treatment time were designated as A-NT4, A-NT8, and A-NT24, respectively.

Acylation of MWNTs and esterification of acylated MWNTs with PUD

About 0.2 g of as-prepared MWNT-COOH was firstly sonicated in 20 mL of EA and then reacted with 50 mL of $SOCl_2$ for 24 h under reflux. The residual $SOCl_2$ and EA was removed by rotary evaporation, giving acyl chloride-functionalized MWNTs (MWNT-COCl). The MWNT-COCl was washed with purified EA three times. The as-produced MWNT-COCl was immediately reacted with 1.0 g of PUD at 100°C for 24 h, obtaining PUD-grafted MWNTs after repeated centrifugation at 7500 rpm, washing, and vacuum drying. The products prepared from A-NT8 and A-NT24 were designated as NT8D and NT24D, respectively.

Nanocomposite films

In a typical experiment, the matrix PUD (4 g) was dissolved in DMF (16 mL) to form a homogeneous solution. To the solution was added dropwise a DMF solution of PUD-functionalized carbon nanotubes (NT8D) under constant stirring. The resulting

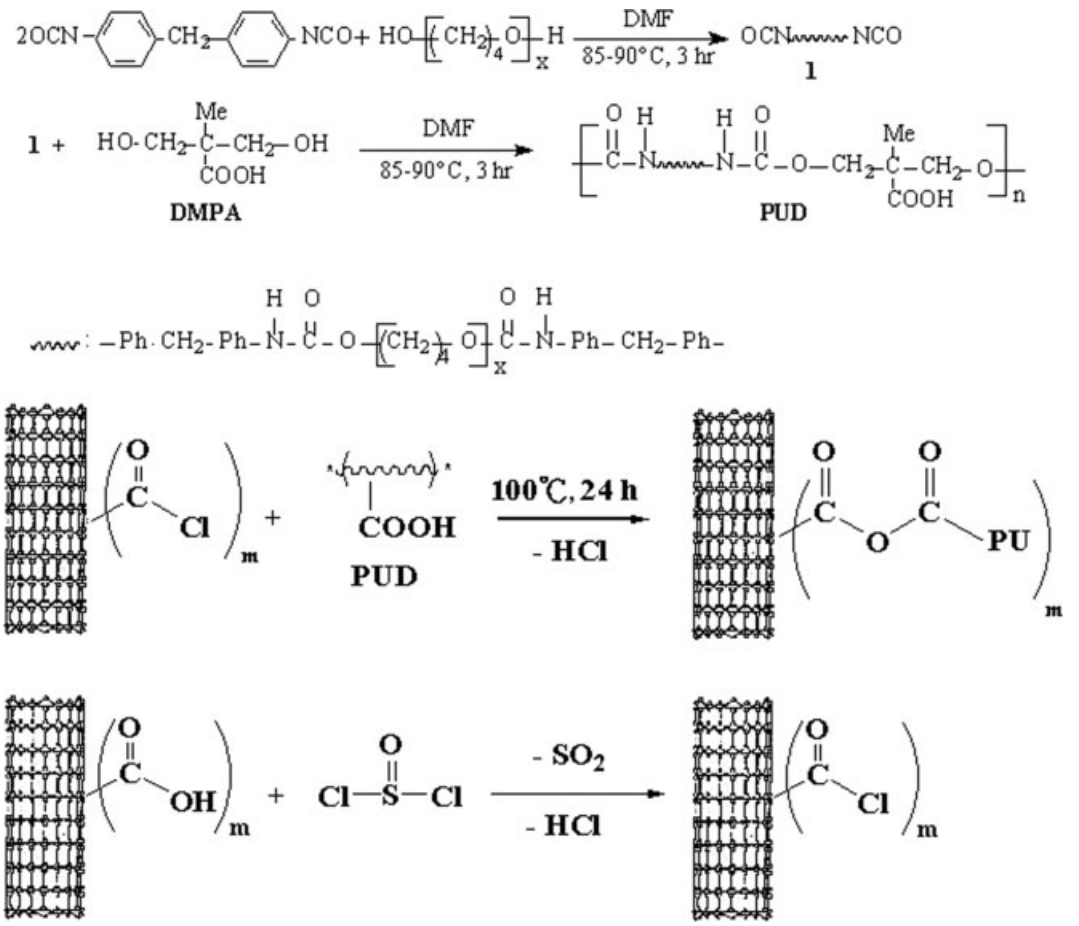

Scheme 1 Reaction pathway for the functionalization of MWNTs with segmented polyurethanes (PUD).

solution was cast onto a glass substrate and dried at 50°C for 48 h. In this study, three different compositions, i.e., 1, 5, and 10 wt % of NT8D based on the original amount of PUD (4 g) were prepared for comparison.

Characterization

Infrared spectra of samples were obtained using a Bio-Rad FTS 165 Fourier transform infrared spectrometer. The spectra were obtained over the frequency range of 4000–400 cm^{-1} at a resolution of 4 cm^{-1}.

Raman spectra was obtained with a Triax 550 spectrophotometer (Japan), an excitation wavelength of a 514-nm line from an argon laser was used.

XPS surface analysis was carried out using a VG Instruments X-ray photoelectron spectrometer. Mg-Kα radiation was used as the X-ray source and the photoelectron peaks (in the wide-scan spectra) from the samples were numerically fitted using Lorentzian curves with an integral background subtraction and analyzed at an angle of 45° to the surface. The adventitious C(1s) signal at 284.6 eV was used to calibrate the charge-shifted energy scale.

Wide-angle X-ray diffractograms (WAXD) were obtained on a Rigaku Geiger Flex D-Max III, using Ni-filtered Cu-Kα radiation (40 kV, 15 mA); the scanning rate was 4°/min.

Thermogravimetric analysis (TGA) experiments were carried out on samples placed in a platinum sample pan using a TA Instruments SDT-2960 analyzer. Products ranging from 4 to 5 mg were loaded into the platinum pan and sealed in the sample chamber. The samples were heated from 50 to 900°C under a nitrogen atmosphere at a heating rate of 10°C/min.

Scanning electron microscopy (SEM) images were recorded using a Hitachi *S*-4800 field-emission microscope, and the samples were precoated with a homogeneous gold layer by sputtering technology.

Dynamic mechanical analysis (DMA) was performed on a Perkin–Elmer DMA7e unit with an operating temperature range from −100 to 50°C. The heating rate was set at 5°C/min. The sample size was approximately 5.5 × 1.5 × 0.5 mm^3.

Stress–strain data of nanocomposite films were obtained using a Universal Testing Machine (Shimadzu AGS-500A Series) with a 10 kg load cell and film grips. The crosshead speed was 20 mm/min.

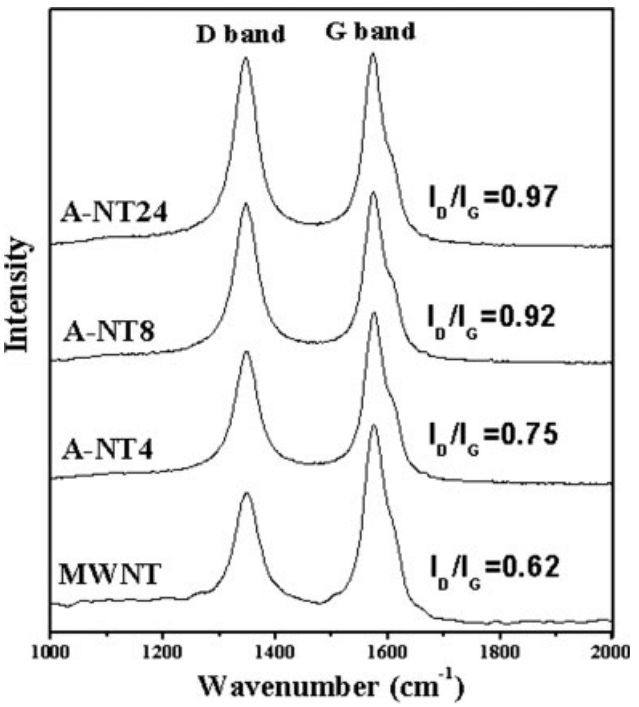

Figure 1 Raman spectra of crude MWNTs and acid-treated MWNTs with different treatment times.

Measurements were made at room temperature using a 1.2 × 0.4 cm^2 dumbbell sample.

RESULTS AND DISCUSSION

Characterization of acid-treated MWNTs

Raman spectroscopy is a powerful tool to characterize the functionalized CNTs. As shown in Figure 1 (514 nm excitation), the crude MWNTs and acid-treated MWNT samples (A-NT4, A-NT8, and A-NT24) show well-defined Raman bands at 1347 and 1574 cm^{-1}. The position of the first strong peak at 1347 cm^{-1} is due to the D band described in the literature, which is caused by the induction of significant defects or disorder in these nanostructures.[23,36] The second strong band at 1574 cm^{-1} is assigned to Raman-active E_{2g} mode (G-band stretching), analogous to that of graphite.[23,36] The frequency, intensity, and line width of the bands at 1347 and 1574 cm^{-1} of the A-NTs are similar to those of crude MWNTs. The intensity of the D band increased with increasing acid treatment time, so do D- to G-band intensity ratios (I_D/I_G). These ratios are greater than that of crude MWNTs (~ 0.62). As seen in the figure, the intensity of the D band significantly increase with increasing acid treatment time up to 8 h and then increase only slightly after acid-treated 24 h. This means that the defects or disordered portion increased a little after 8 h of acid treatment. This result significantly provides useful information about the suitable time of acid treatment. On the other hand, the D′-band shown as a shoulder at 1605 cm^{-1}, which is known to be directly affected by the disorder in nanotubes,[37] also exhibits different relative intensities for crude and modified MWNTs. This band can be barely observable in pristine tubes but is clearly detectable after functionalization, indicating an increase in defects along the tube body.

Generally, electron spectroscopy for chemical analysis (i.e., XPS) provides qualitative and quantitative information about the elemental composition of matter; particularly, it is very useful for the characterization of a polymer surfaces.[38,39] Figure 2 shows the C(1s) and O(1s) spectra of the MWNTs treated with mixed acid for various times. The XPS C(1s) spectrum of the crude MWNT exhibits a sharp peak at 284.1 eV, which is assigned to an sp^2 carbon.[38,39] The XPS O(1s) spectrum of the crude MWNTs shows a peak near 533.0 eV, corresponding to ether-type oxygen (—C—O—) of COOH.[38,39] From the O(1s) area ratio determined by the XPS, the atomic concentration of oxygen for A-NT4, A-NT8, and A-NT24 are 11.1, 14.6, and 16.8 atomic %, respectively. Conversely, with increasing acid treatment time of the MWNTs, the atomic concentration of carbon decreases from 88.9 to 83.2 atomic percentage. Therefore, the O/C ratio increases with increasing acid treatment time. The higher surface oxygen content for the carboxylic acid functionalized MWNTs, in comparison with that of the as-received materials, is evidence of COOH groups on the MWNT surface.

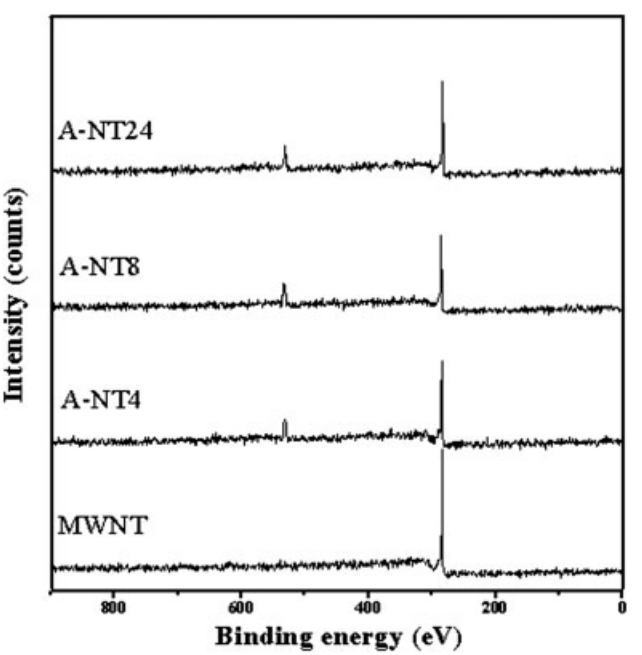

Figure 2 XPS spectra of crude MWNTs and acid-treated MWNTs with different treatment times.

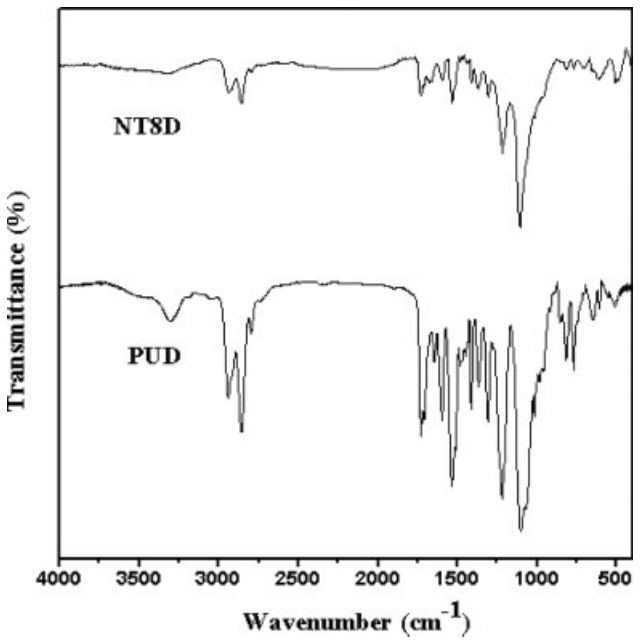

Figure 3 FTIR spectra of PUD and NT8D.

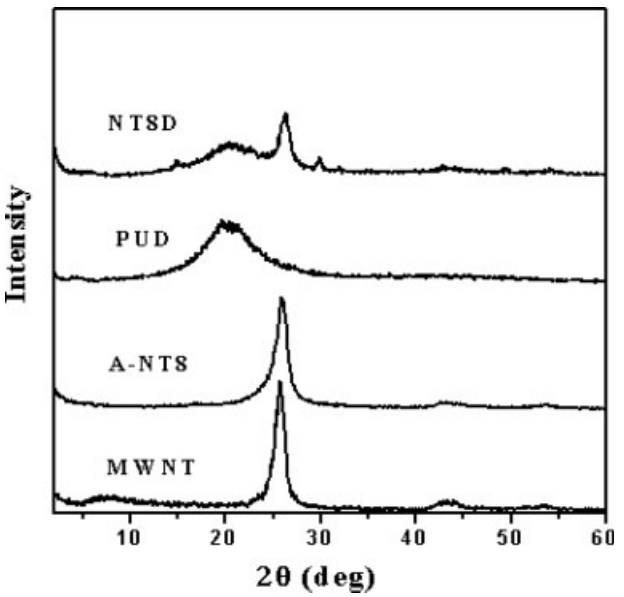

Figure 4 X-ray diffraction patterns of MWNT, A-NT8, PUD, and NT8D.

Synthesis and characterization of MWNT-PUD

The functionalization of CNTs by grafting polyurethane to the sidewalls of MWNTs is shown in Scheme 1. Though lots of literatures related to covalent functionalization of CNTs by polymers, the investigation of grafting polyurethane onto the sidewalls of CNTs by ''grafting to'' approach has rarely been mentioned. In this article, we only focus on the preparation and characterization of MWNT-PUD nanohybrids. The chemical structure of the resulting nanohybrids is also illustrated in Scheme 1. It is noteworthy that the adsorbed polyurethane can be efficiently removed from the products by filtration and washing as mentioned in the Experimental Section. From IR measurement for the upper layer of DMF solution, collected by centrifuging (1 h at a rate of 7500 rpm) of MWNT-PUD dispersed in the DMF, showed that no polyurethane signals appeared in the spectrum. This indicates that the adsorbed polymer quantity is negligible. Therefore, the ''grafting to'' approach presented here promised the grafting of polyurethanes onto CNT surfaces with some extent of control.

Since characterization of PUD has been published elsewhere,[35] this part will only concern about the characterization of MWNT-PUD. The molecular composition of the resulting MWNT-polyurethane nanohybrids was confirmed by FTIR and WAXD measurements. Since the results of NT8D and NT24D are similar, the IR spectrum and XRD pattern of NT8D are shown as a representative example in Figures 3 and 4, respectively. For NT8D, the characteristic absorption peaks of polyurethane such as —CH_2—, NHCOO—, C—O—C, clearly appear at 2930/2853, 1730, 1100 cm^{-1}, respectively. The benzene-ring C=C absorption peak from MDI is at $\sim$ 1600 cm^{-1}, while the peaks at 1530 and 1220 cm^{-1} correspond to C—N of urethane groups (Fig. 3). This spectrum clearly shows that PUD has been grafted to MWNTs successfully.

The X-ray diffraction pattern for MWNT, A-NT8, PUD, and NT8D are shown in Figure 4. Their distances were calculated with Bragg's law. The broad band for PUD centered at $2\theta = 20.4^\circ$ from which a spacing of 4.35 Å can be calculated, is assigned to polyurethane interchain spacings. For MWNT and

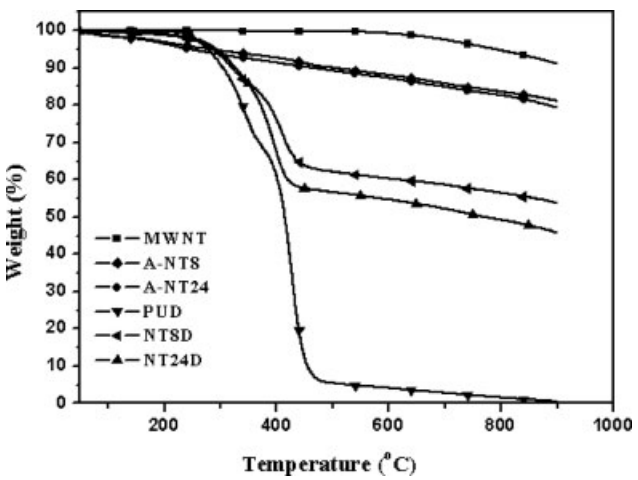

Figure 5 TGA weight loss curves of crude MWNTs, acid-treated MWNTs, and PU-functionalized MWNTs under a nitrogen atmosphere.

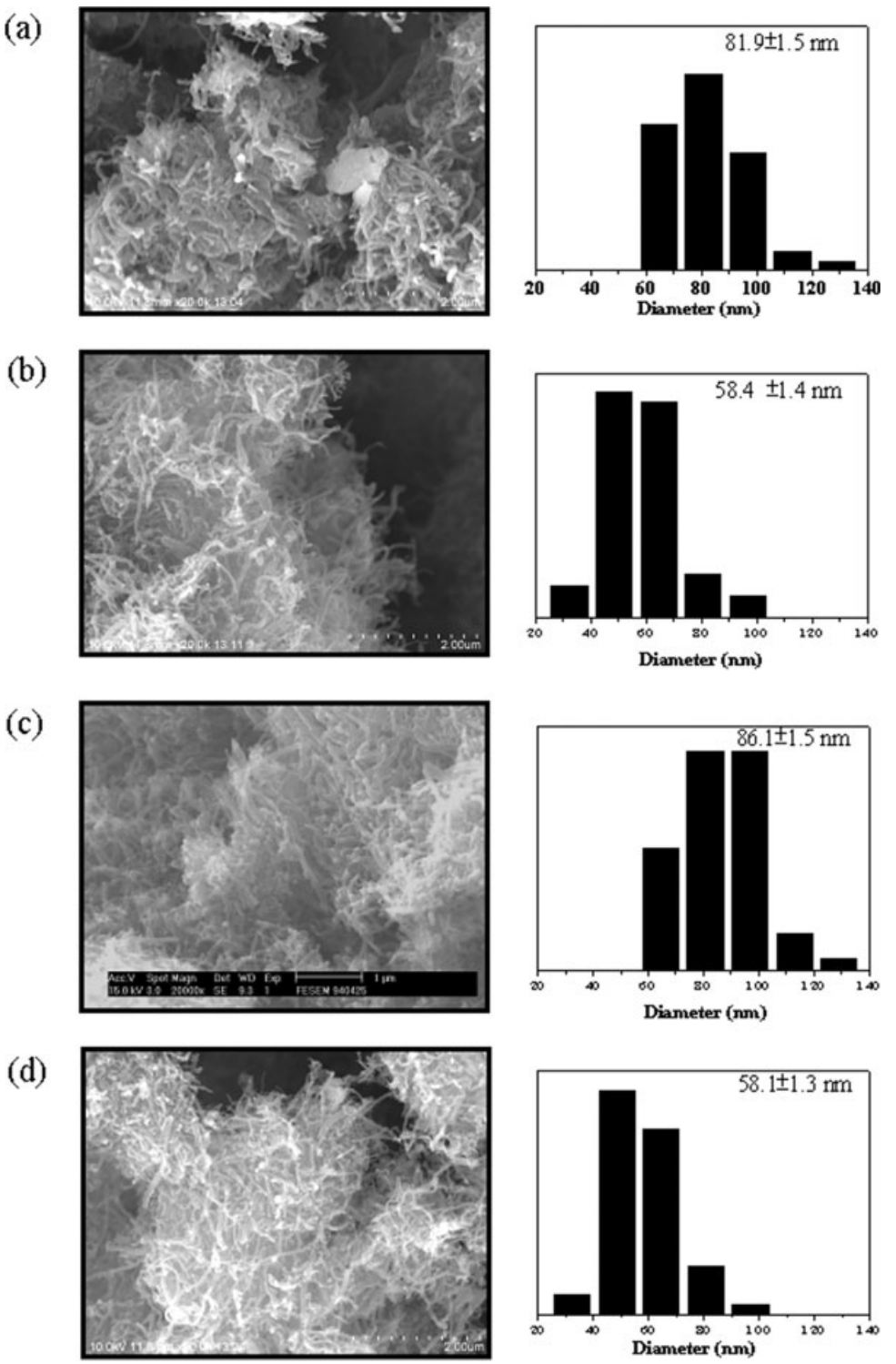

Figure 6 SEM micrographs of PU-functionalized and chemically defunctionalized MWNT samples. (a) NT8D. (b) NT8D defunctionalized at 900°C for 2 h. (c) NT24D. (d) NT24D defunctionalized at 900°C for 2 h.

A-NT8, a sharp signal can be seen at $2\theta = 26.2^\circ$, corresponding to a spacing of 3.40 Å. This signal has been reported as the diffraction signature of the distance between walls in MWNTs.[40,41] Furthermore, the signal at $2\theta = 43.4^\circ$ ($d = 2.08$ Å) is attributed to the MWNT interwall spacing as well.[42] The two MWNT interwall signals discussed ($2\theta = 26.2^\circ$ and $2\theta = 43.4^\circ$) have been determined to be the reflections of (002) and (004) graphitic planes, respectively.[42] Finally, the signals at lower angles ($2\theta = 7.7^\circ$) are due

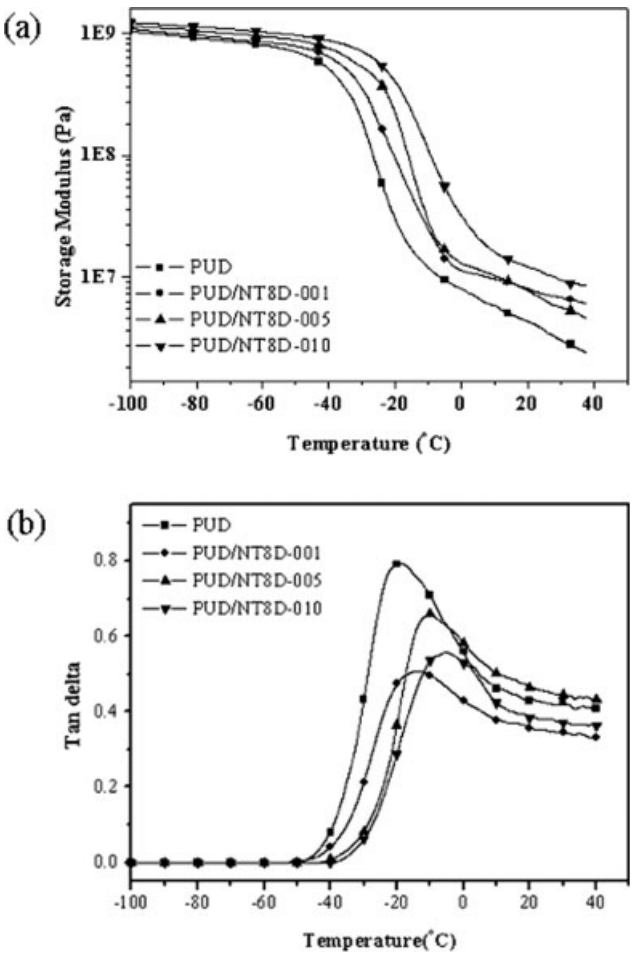

Figure 7 Temperature dependence of (a) storage modulus (E'), (b) loss tangent (tan δ) for PUD and PUD/NT8D composite films.

to low-angle scattering of amorphous carbon and graphitic particles.[43] For NT8D the X-ray diffraction shows the characteristic broad peak of PUD and the strong peaks of MWNT. This fact also confirms that the preparation of MWNT-PUD was successful.

In general, polymer-functionalized CNTs would show much higher solubility or better dispersibility as compared with pristine nanotubes. Herein, as polyurethane is polar, our resulting samples of MWNT-polyurethane are readily dispersed in polar organic solvents, such as DMSO, DMF, 1-methyl-2-pyrrolidinone (NMP), and *N*,*N*-dimethyl acetamide (DMAc), etc. The dark-colored solutions from the soluble samples are stable, without any precipitations over time.

Thermal analysis and morphology of the resulting MWNT-polyurethane nanohybrids

To obtain the grafted amount of polyurethane on MWNTs, thermal analysis of MWNT-PUD prepared from MWNTs with different acid treatment time (8 and 24 h) were carried out. The thermal stability for crude MWNTs and functionalized MWNTs in nitrogen is illustrated in Figure 5. As seen in the figure, the TGA curves display a two-step degradation mechanism for PUD, NT8D, and NT24D, which is quite different with the one-step degradation mechanism of MWNT and A-NTs. It is obvious that PUD has been grafted onto the sidewalls of MWNTs. In the MWNT-COOH case, there is a continuous but not very obvious decrease in weight, which is typical for acid functionalized MWNTs. In comparison with the curves of MWNTs and acid-treated MWNTs, the rapid degradation stage in NT8D and NT24D may arise because of the decomposition of grafted PUD. When compared with crude MWNTs, the functionalized acid amount could be calculated by the subtraction of char yields of A-NTs from MWNT. Thus, the functionalized acid amounts for A-NT8 and A-NT24 are 10.0 and 12.2%, respectively. In addition, the grafted amounts of PUD were also obtained. According to the TGA traces, the PUD contents in the NT8D and NT24D samples are approximately 27.7% and 33.4%, respectively. It was found that the longer acid treatment time results in a higher grafted amount of PUD. This further confirms the successful functionalization of MWNTs.

The fine nanostructures of the as-prepared MWNT-polyurethane nanohybrides were investigated by SEM. As shown in Figure 6(a,c), MWNTs were coated by a layer of polymer chains. From the SEM images of the MWNT-PUD samples, we can clearly discern that the higher the quantity of the grafted polymer, the thicker the polymer shell. The calculated diameters for NT8D and NT24D are $\sim$ 81.9 and 86.1 nm, respectively. After heat treatment of NT8D and NT24D at 900°C for 2 h, the defunctionalized tube surfaces are relatively smooth and clean [Fig. 6(b,d)], obviously different from that of the polyurethane-functionalized MWNTs. The tube diameters are $\sim$ 58.4 and 58.1 nm, respectively, being close to the diameter of pristine MWNTs.

Nanocomposites

In this research, MWNTs were functionlalized with PUD to be more compatible with the polymer matrix PUD of the nanocomposites. The common solubility of the PUD-functionalized carbon nanotubes and the matrix PUD also makes the solution casting easier. The compatibility of the PUD-functionalized carbon nanotubes with polyurethane and the dispersion of the nanotubes in polyurethane matrix were evaluated via the fabrication of nanocomposite thin films. In a typical experiment, a calculated amount of NT8D (w/w) based on PUD matrix was dissolved in DMF and added to a PUD solution. For comparison, 1, 5,

TABLE I
Composition and Physical Properties of PUD and PUD/NT8D Composite Films

Specimens	Composition (wt %) PUD/NT8D	T_g (°C) (soft segment)	Storage modulus at −40°C (E')	Tensile strength (KPa)	Elongation at break(%)
PUD	100/0	−20	5.13E8	377	190
PUD/NT8D-001	100/1	−14	6.45E8	614	170
PUD/NT8D-005	100/5	−10	7.54E8	934	155
PUD/NT8D-010	100/10	−5	8.78E8	1167	115

and 10 wt % of NT8D based on 100 wt % of PUD were used as the reinforcing fillers. They were designated as NT8D-001, NT8D-005, and NT8D-010, respectively. According to TGA results, the actual contents of carbon nanotubes in the above three nanocomposites are ~ 0.72, 3.62, and 7.23 wt %. The resulting composite solution was allowed to settle overnight and then centrifuged to remove any residual insoluble species, followed by being concentrated to attain the desired viscosity. The viscous but transparent solution was used for the casting of a thin film. The polyurethane-MWNT composite thin film thus obtained is transparent with a high optical quality. The successful fabrication of optically high-quality nanocomposite thin films reflects the excellent compatibility of the PUD-functionalized carbon nanotubes with polyurethane. It also serves as initial evidence for the notion that functionalized carbon nanotubes can be dispersed homogeneously into polymeric matrices. The mechanical properties of the nanocomposites were analyzed with dynamic mechanical analysis (DMA). The soft segment T_gs of the three composite films were also obtained from loss tangent of DMA. As shown in Figure 7, the dynamic storage modulus (E') and loss tangent (tan δ) of the PUD/MWNT-PUD nanocomposite films show enhanced mechanical properties and increased soft segment T_g. The results of soft segment T_g of the three composites are listed in Table I. The enhanced E' of PUD/NT8D nanocomposites are induced from the stiffening effect of the CNTs. E' of the PUD/NT8D nanocomposite films prepared in this study increases with increasing NT8D content, which is due to the stiffening effect of the NT8D. However, in comparison with the E' values of PUD, the increased amounts of E' of the three nanocomposites are not very satisfactory. Since the load acting on the matrix has to be transferred to the reinforcement via the interface. This may be attributed to a weak interface arising from a weak adhesion between the reinforcement and the matrix. The detail bonding mechanism at the reinforcement-matrix interface is beyond the scope of this article. For the convenience of comparison, data of E' at −40°C are also shown in Table I. Moreover, with increasing NT8D content, the glass-transition temperature of the soft segments of the PUD/NT8D nanocomposite films shifts from −20 to −5°C. The increase of soft segment T_g is attributed to the constraint of polyurethane chains by carbon nanotubes. This means that MWNT-PUDs are compatible with the amorphous regions of the soft segments in PUD matrix.

Figure 8 shows the stress–strain curves of the PUD film and PUD/NT8D nanocomposite films. The results of tensile strength and elongation at break of the PUD/NT8D nanocomposite films are also summarized in Table I. The tensile strengths of the nanocomposite films are enhanced with 1–10 wt % loading of NT8D compared with the corresponding value of the original PUD film. As the NT8D content increased from 1 to 10 wt %, the tensile strength of the PUD/NT8D nanocomposite films increases from 614 to 1167 KPa, corresponding to an increasing ratio of 63 to 210%; however, the elongation at break (% of strain) decreased from 170 to 115%. These increases in the PUD/NT8D nanocomposites are due to the reinforcing effect of MWNT-PUDs in the PUD matrix.

CONCLUSIONS

MWNTs were covalently functionalized with segmented polyurethanes using the ''grafting to'' tech-

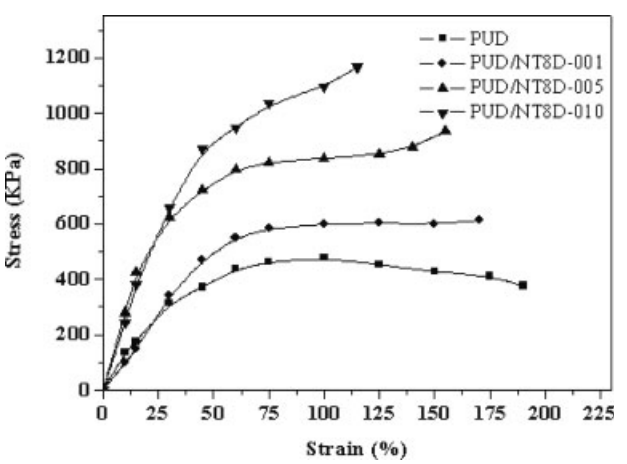

Figure 8 Stress–strain curves for PUD and PUD/NT8D composite films.

nique. The segmented polyurethane (PUD) with carboxyl groups pendant on the polymer backbone were synthesized by the conventional prepolymer technique. The oxidized MWNTs (MWNT-COOH) were converted into acyl chloride functionalized MWNTs (MWNT-COCl) by reaction with neat thionyl chloride ($SOCl_2$) and reacting them with polyurethane to prepare the MWNT-polyurethane. The Raman spectra of the crude MWNTs and A-NTs have well-defined Raman bands at 1347 cm^{-1} (D band) and 1574 cm^{-1} (G band). The intensity of D band significantly increases with increasing acid treatment time. By XPS analysis, the presence of O(1s) for A-NTs indicates the successful oxidization of MWNTs. The structures of the as-prepared MWNT-PUD nanohybrids were characterized with FTIR and XRD. From the characteristic peaks of PUD shown in both spectra, PUD has been grafted to the surfaces of MWNTs successfully. TGA results indicate that the longer acid treatment time, the higher grafted amount of PUD. SEM investigations gave direct evidence of the nanostructures of the MWNT-PUD hybrids. The nanohybrids are well dispersed in the same solvents for neat PU, thus allowing the intimate mixing of the functionalized nanotubes with the matrix polymer for the preparation of nanocomposites. Dynamic mechanical analysis shows the storage modulus and the soft segment T_g of the nanocomposites increase with increasing MWNT-PUD content. The tensile strengths of the nanocomposite films with different weight ratio loading of MWNT-PUD are enhanced by about 63–210%, compared with the corresponding value of the original PUD film.

References

1. Dresselhaus, M. S.; Dresselhaus, G.; Eklund, P. C. Science of Fullerenes and Carbon Nanotubes; Academic Press: New York, 1996.
2. Saito, R.; Dresselhaus, M. S.; Dresselhaus, G. Physical Properties of Carbon Nanotubes; Imperial College Press: London, 1998.
3. Kong, J.; Franklin, N. R.; Zhou, C.; Chaplin, M. G.; Peng, S.; Cho, K.; Dai, H. Science 2000, 287, 622.
4. Tans, S. J.; Verschueren, R. M.; Dekker, C. Nature 1998, 393, 49.
5. Baughman, R. H.; Zakhidov, A. A.; de Heer, W. A. Science 2002, 297, 787.
6. Chen, J.; Hamon, M. A.; Hu, H.; Chen, Y.; Rao, A. M.; Eklund, P. C.; Haddon, R. C. Science 1998, 282, 95.
7. Chen, X.; Armes, S. P. Adv Mater 2003, 15, 1558.
8. Hirsch, A. Angew Chem Int Ed Engl 2002, 41, 1853.
9. Sun, Y. P.; Fu, K.; Lin, Y.; Huang, W. Acc Chem Res 2002, 35, 1096.
10. Czerw, R.; Guo, Z.; Ajayan, P. M.; Sun, Y. P.; Carroll, D. L. Nano Lett 2001, 1, 423.
11. Qin, S.; Qin, D.; Ford, W. T.; Resasco, D. E.; Herrera, J. E. Macromolecules 2004, 37, 752.
12. Lin, Y.; Zhou, B.; Shiral Fernando, K. A.; Liu, P.; Allard, L. F.; Sun, Y. P. Macromolecules 2003, 36, 7199.
13. Shaffer, M. S. P.; Koziol, K. Chem Commun 2002, 2074.
14. Wu, W.; Zhang, S.; Li, Y.; Li, J.; Liu, L.; Qin, Y.; Guo, Z. X.; Dai, L.; Ye, C.; Zhu, D. Macromolecules 2003, 36, 6286.
15. Kong, H.; Gao, C.; Yan, D. J Am Chem Soc 2004, 126, 412.
16. Liu, I.; Huang, H.; Chang, H. C.; Tsai, H.; Hsu, C.; Tsiang, R. C. Macromolecules 2004, 37, 283.
17. Ajayan, P. M.; Stephan, O.; Colliex, C.; Trauth, D. Science 1994, 265, 1212.
18. Ajayan, P. M.; Schadler, L. S.; Giannaris, C.; Rubio, A. Adv Mater 2000, 12, 750.
19. Ago, H.; Petritsch, K.; Shaffer, M. S. P.; Windle, A. H.; Friend, R. H. Adv Mater 1999, 11, 1281.
20. Mitchell, C. A.; Bahr, J. L.; Arepalli, S.; Tour, J. M.; Krishnamoorti, R. Macromolecules 2002, 35, 8825.
21. Hill, D. E.; Lin, Y.; Rao, A. M.; Allard, L. F.; Sun, Y. P. Macromolecules 2002, 35, 9466.
22. Xu, Y.; Gao, C.; Kong, H.; Yan, D.; Jin, Y. Z.; Watts, P. C. P. Macromolecules 2004, 37, 8846.
23. Ruan, S. L.; Gao, P.; Yang, X. G.; Yu, T. X. Polymer 2003, 44, 5643.
24. Tang, W.; Santare, M. H.; Advani, S. G. Carbon 2003, 41, 2779.
25. Gordeyev, S. A.; Macedo, F. J.; Ferreira, J. A.; Hattum, F. W. J.; Bernardo, C. C. Phys B Condens Matter 2000, 279, 33.
26. Jia, Z.; Wang, Z.; Xu, C.; Liang, J.; Wei, B.; Wu, D.; Zhu, S. Mater Sci Eng A 1999, 271, 395.
27. Jin, Z.; Pramoda, K. P.; Xu, G.; Goh, S. H. Chem Phys Lett 2001, 337, 43.
28. Quan, D.; Dickey, E. C.; Andrews, R.; Rantell, T. Appl Phys Lett 2000, 76, 2868.
29. Andrews, R.; Jaques, D.; Rao, A. M.; Rantell, T.; Derbyshire, F.; Chen, Y.; Chen, J.; Haddon, R. C. Appl Phys Lett 1999, 75, 1329.
30. Schadler, L. S.; Ciannaris, S. C.; Ajayan, P. M. Appl Phys Lett 1998, 73, 3842.
31. Park, J. M.; Kim, D. S.; Lee, J. R.; Kim, T. W. Mater Sci Eng C 2003, 23, 971.
32. Gao, C.; Jin, Y. Z.; Kong, H.; Whitby, R. L. D.; Acquah, S. F. A.; Chen, G. Y.; Qian, H.; Silva, A. H. S. R. P.; Henley, S.; Fearon, P.; Kroto, H. W.; Walton, D. R. M. J Phys Chem B 2005, 109, 11925.
33. Kwon, J.; Kim, H. J Polym Sci Part A: Polym Chem 2005, 43, 3973.
34. Kwon, J.; Kim, H. J Appl Polym Sci 2005, 96, 595.
35. Huang, F. J.; Wang, T. L. J Polym Sci Part A: Polym Chem 2004, 42, 290.
36. Chapelle, M. L.; Lefrant, S.; Journet, C.; Maser, W.; Bernier, P.; Loiseau, A. Carbon 1998, 36, 705.
37. Jorio, A.; Pimenta, M. A.; Souza Filho, A. G.; Saito, R.; Dresselhaus, G.; Dresselhaus, M. S. New J Phys 2003, 5, 139.1.
38. Skoog, D. A.; Holler, F. J. Principles of Instrumental Analysis, 5th ed.; Saunders: Philadelphia; 1992.
39. Kim, E. Y.; Kong, J. S.; An, S. K.; Kim, H. D. J Adhes Sci Technol 2000, 14, 1119.
40. Hilding, J.; Grulke, E. A.; Zhang, Z. G.; Lockwood, F. J Dispersion Sci Technol 2003, 24, 1.
41. Saito, Y.; Yoshikawa, T.; Bandow, S.; Tomita, M.; Hayashi, T. Phys Rev B 1993, 1907, 48.
42. Dore, J.; Burian, A.; Tomita, S. Acta Phys Pol A 2000, 98, 495.
43. Duclaux, L.; Salvetat, J. P.; Lauginie, P.; Cacciaguera, T.; Faugere, A. M.; Goze-Bac, C.; Bernier, P. J Phys Chem Solids 2003, 64, 571.